

Supplementary Materials for

Irisin protects mitochondria function during pulmonary ischemia/reperfusion injury

Ken Chen, Zaicheng Xu, Yukai Liu, Zhen Wang, Yu Li, Xuefei Xu, Caiyu Chen, Tianyang Xia, Qiao Liao, Yonggang Yao, Cindy Zeng, Duofen He, Yongjian Yang, Tao Tan, Jianxun Yi, Jingsong Zhou, Hua Zhu, Jianjie Ma,* Chunyu Zeng*

*Corresponding author. Email: chunyuZeng01@163.com (C.Z.); jianjie.ma@osumc.edu (J.M.)

Published 29 November 2017, *Sci. Transl. Med.* **9**, eaao6298 (2017)
DOI: 10.1126/scitranslmed.aao6298

The PDF file includes:

- Fig. S1. Specificity of irisin antibody and absence of endogenous irisin expression in lung epithelial cells.
- Fig. S2. Mass spectrogram profile of irisin peptide.
- Fig. S3. Irisin expression in lung tissues from sham-treated mice after RIPC.
- Fig. S4. Irisin expression in mouse lung tissues at different time points after RIPC, with or without IR injury.
- Fig. S5. OCR of lung tissue from IR-injured mice.
- Fig. S6. Time-dependent accumulation of exogenous irisin in RLE-6TN and BEAS-2B cells.
- Fig. S7. Localization of irisin in mitochondria of cultured lung epithelial cells.
- Fig. S8. Measurement of cell viability and LDH concentration in culture medium derived from lung epithelial cells after AR.
- Fig. S9. Colocalization of irisin and UCP2 in lung epithelial cells.
- Fig. S10. Basal UCP2 expression, inflammation markers, and amount of ROS in WT and *Ucp2*^{-/-} mice.
- Table S1. The characteristics of control and NRDS newborn patients in Fig. 2B.
- Table S2. The characteristics of control and NRDS newborn patients in Fig. 2C.
- Legends for movies S1 to S3

Other Supplementary Material for this manuscript includes the following:

(available at

www.sciencetranslationalmedicine.org/cgi/content/full/9/418/eaao6298/DC1)

Table S3. Original data and *P* values (Excel file).

Movie S1 (.wmv format). Uptake of exogenous irisin into BEAS-2B cells.

Movie S2 (.wmv format). Uptake of exogenous irisin into RLE-6TN cells.

Movie S3 (.wmv format). Uptake of exogenous irisin into A549 cells.

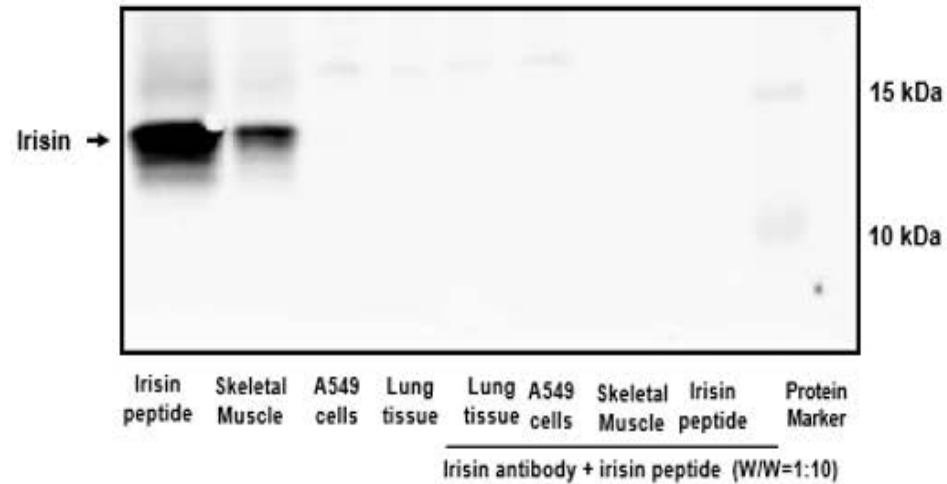
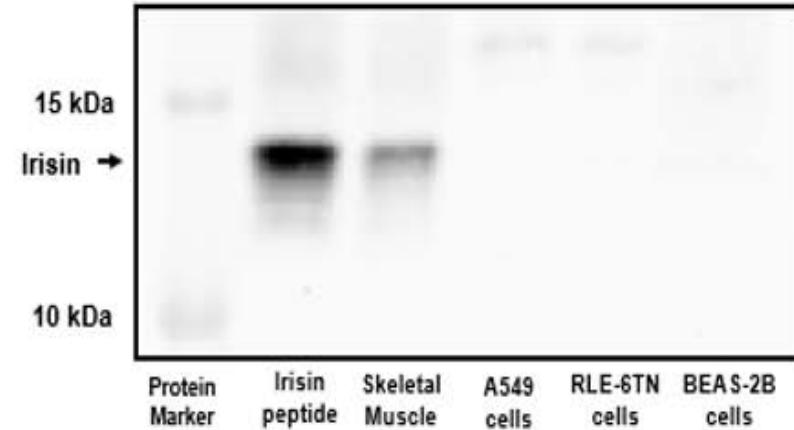
A**B**

Fig. S1. Specificity of irisin antibody and absence of endogenous irisin expression in lung epithelial cells. (A) Proteins (50 µg) from A549, RLE-6TN, and BEAS-2B cells, mouse lung tissue, skeletal muscle, and recombinant irisin peptide (10 µg, Phoenix Pharmaceuticals) were subjected to immunoblotting with anti-irisin antibody (1:500, Phoenix Pharmaceuticals) with or without preincubation with the recombinant irisin peptide (Phoenix Pharmaceuticals, 1:10 w/w incubation for 12 hours). Irisin expression was not detected in lung epithelial cells. The expected 12 kDa irisin band was no longer visible after pre-absorption with recombinant irisin peptide. **(B)** Irisin expression was negative in lung epithelial cells (A549 cells, RLE-6TN cells, BEAS-2B cells; 50 µg protein each). Irisin peptide (10 µg) and protein from skeletal muscle (50 µg) were used as positive controls.

Name	Sequence	m/z	MH+
irisin	FIQEVNTTTR	604.8 Da	1208.6 Da

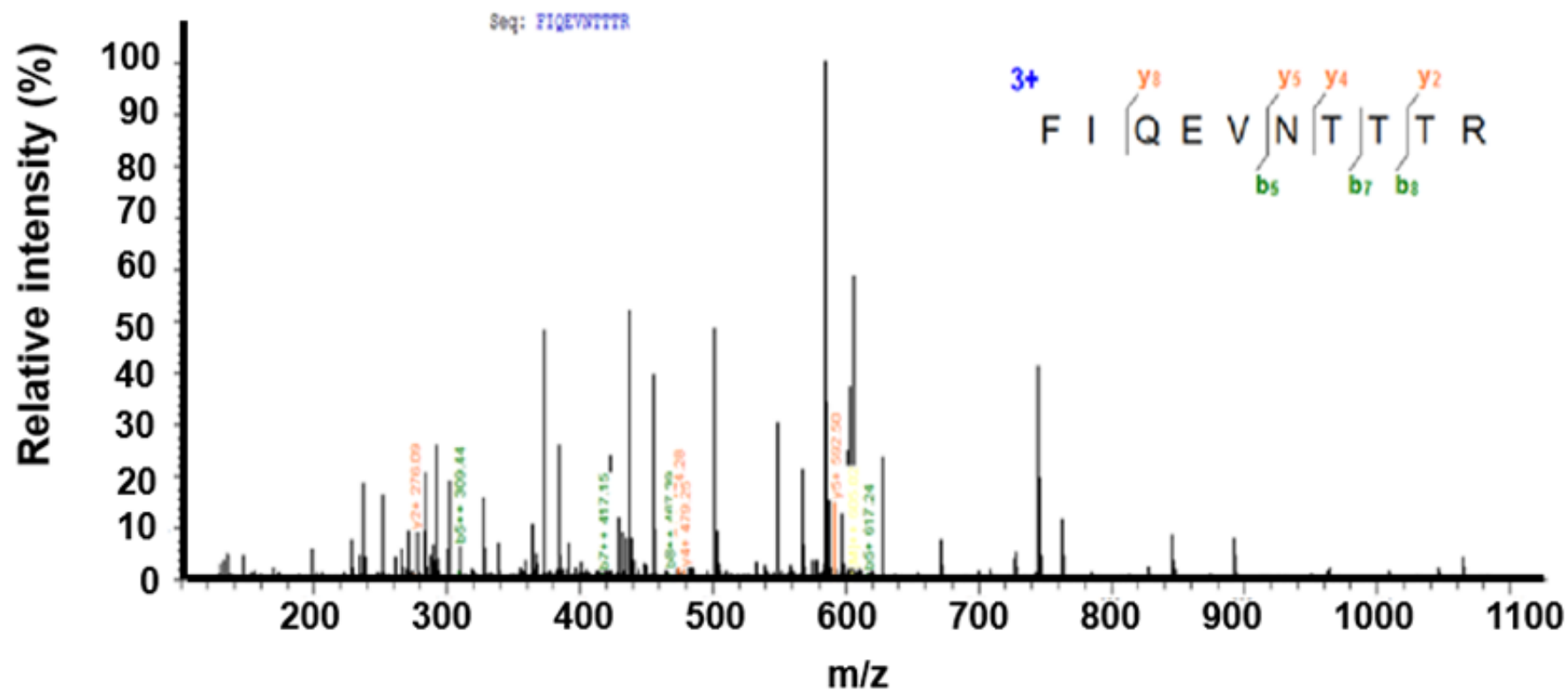


Fig. S2. Mass spectrogram profile of irisin peptide. MS2 spectra indicated the internal tryptic peptide (FIQEVNTTTR) and the b-, y-ion series m/z values, which correspond to the irisin sequence found in serum or BALF samples from infants and mice.

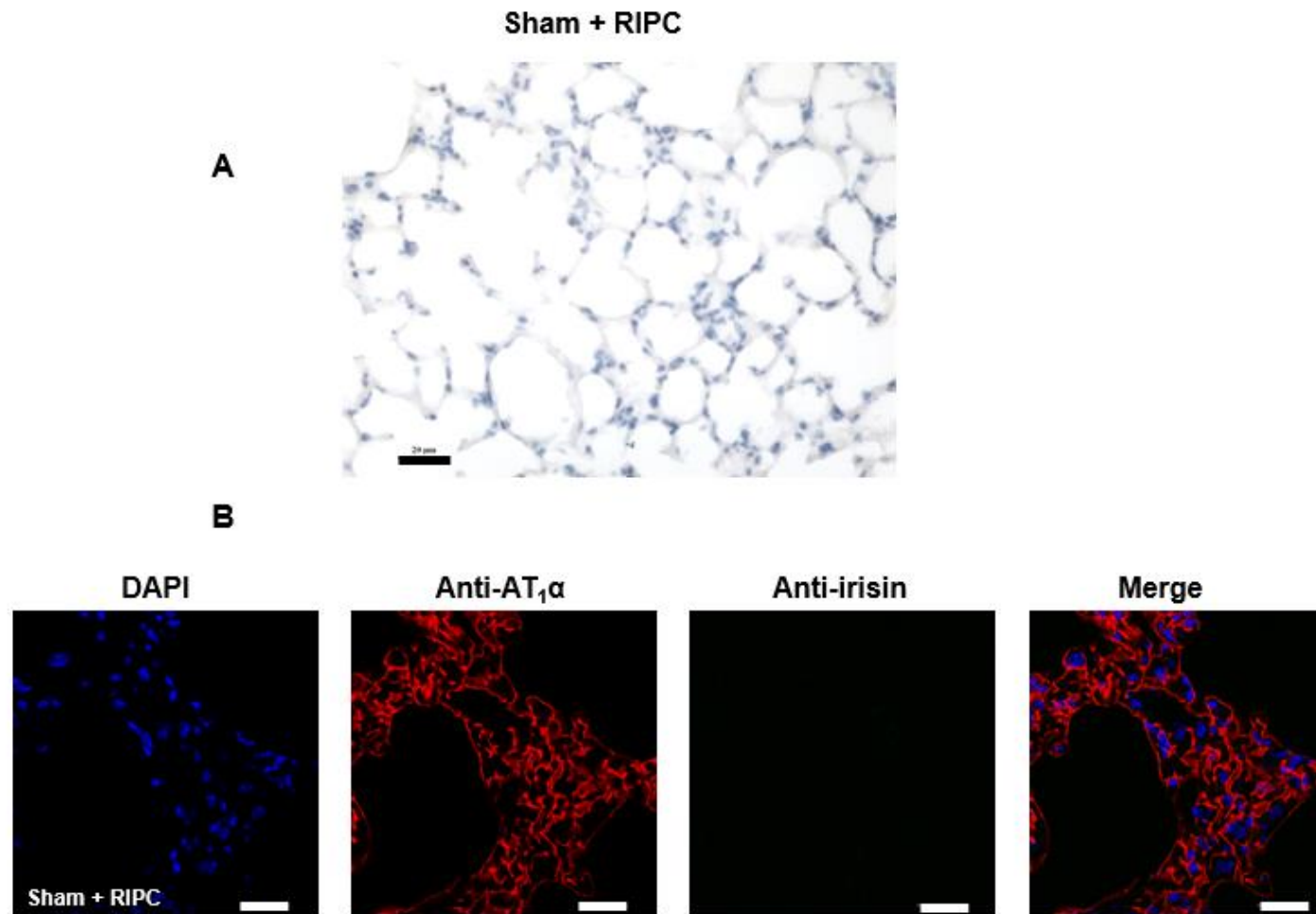


Fig. S3. Irisin expression in lung tissues from sham-treated mice after RIPC. (A) Immunostaining showed that irisin was not detected in the lung tissue from sham-treated mice after RIPC (scale bar = 20 μ m). **(B)** Lung tissue section was immunostained for irisin (green) and AT₁α (red, alveolar type I epithelial cell marker). Irisin staining was not visible. Alveolar epithelial cells did not take up irisin in sham-treated animals after RIPC (scale bar = 20 μ m).

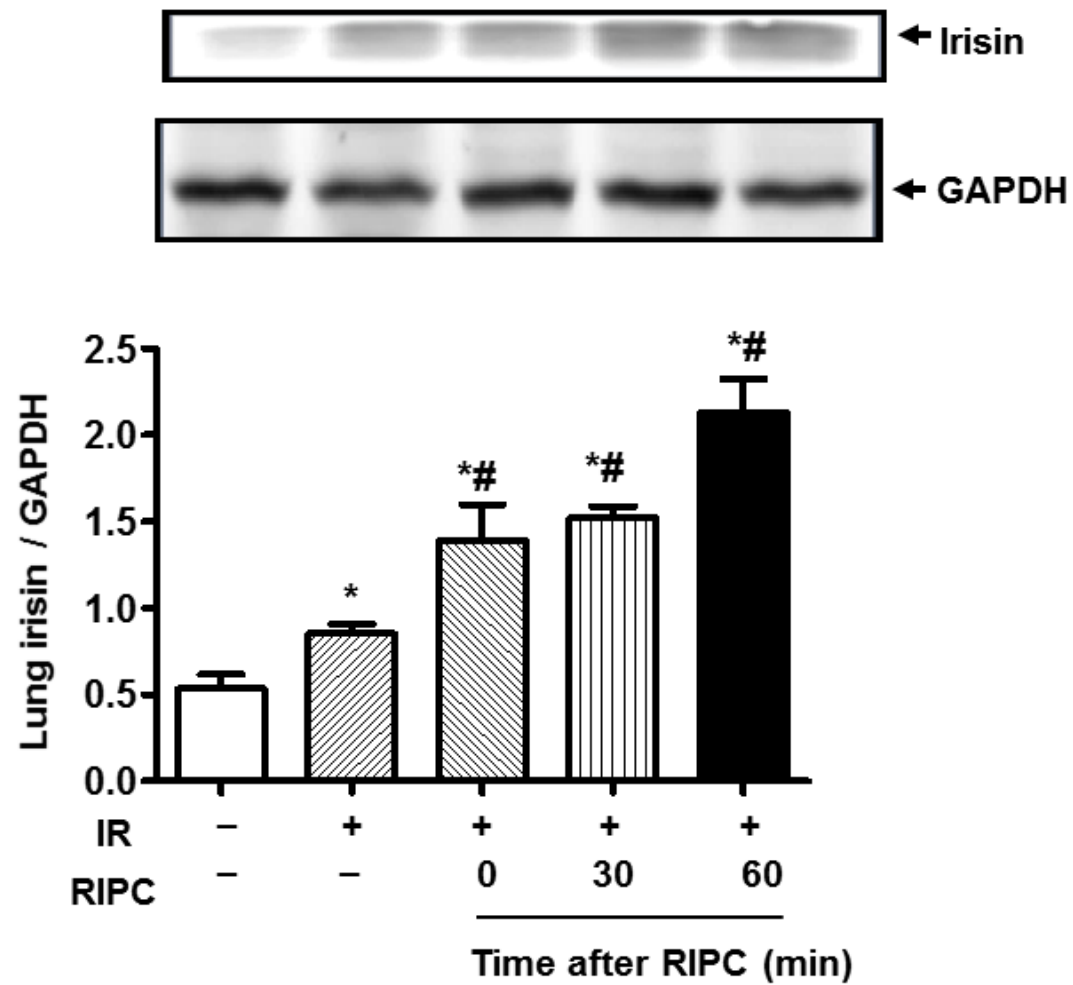


Fig. S4. Irisin expression in mouse lung tissues at different time points after RIPC, with or without IR injury. Irisin expression was measured by Western blot (* $P < 0.05$ vs. non-IR sham group; # $P < 0.05$ vs. IR group; $n = 6$).

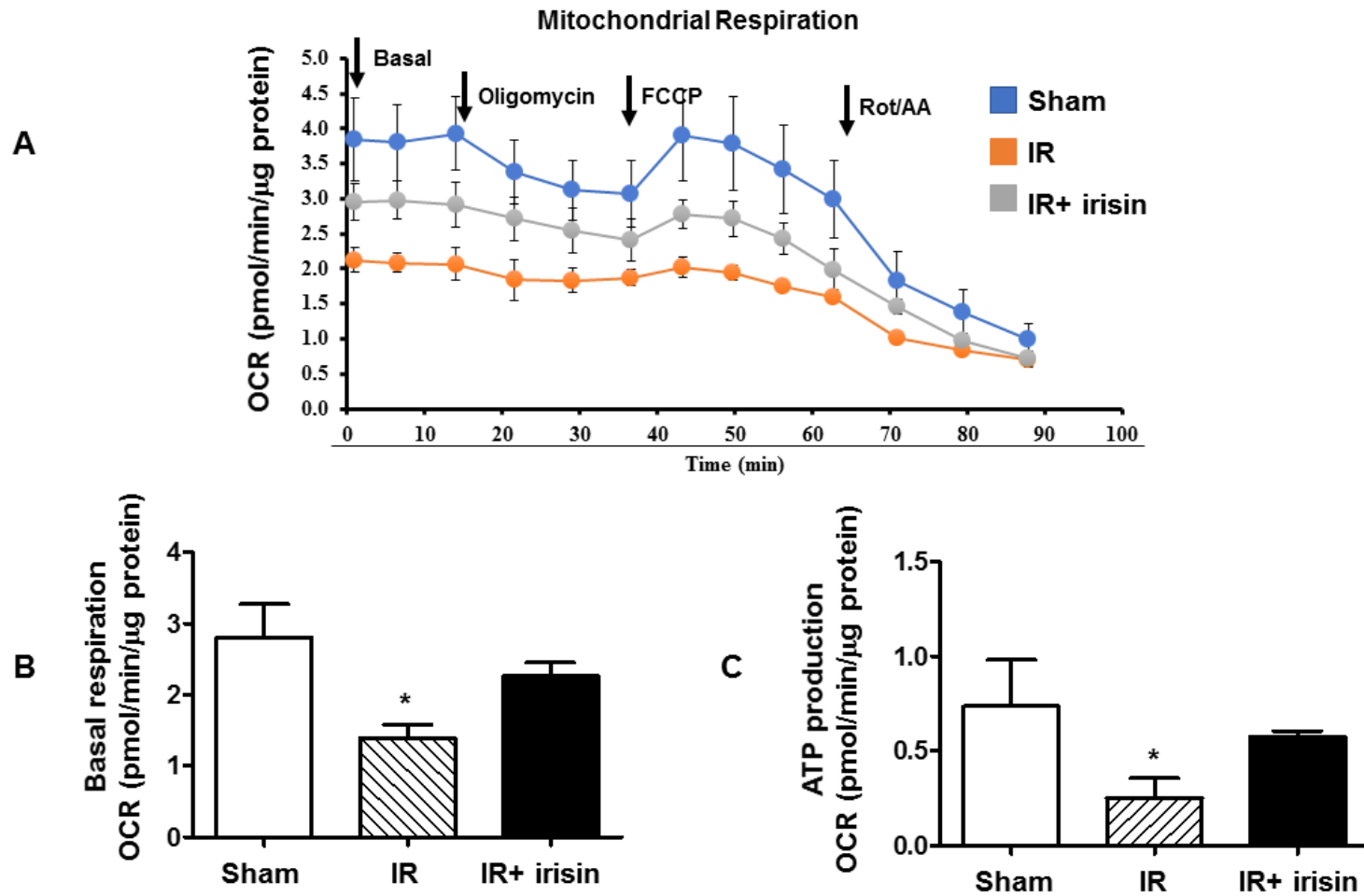


Fig. S5. OCR of lung tissue from IR injured mice. OCR was measured by Seahorse XF24 Mito Stress Test. The changes in OCR (**A**) were assessed after addition of respiratory modulators (arrows): oligomycin (10 μg/ml), FCCP (16 μM), or rotenone /antimycin A (Rot / AA, 3/12 μM). The basal respiration rate (**B**) and ATP production (**C**) were determined by observing how the OCR changes in response to drugs that modulate mitochondrial activity (* $P < 0.05$ vs. others, $n = 3$).

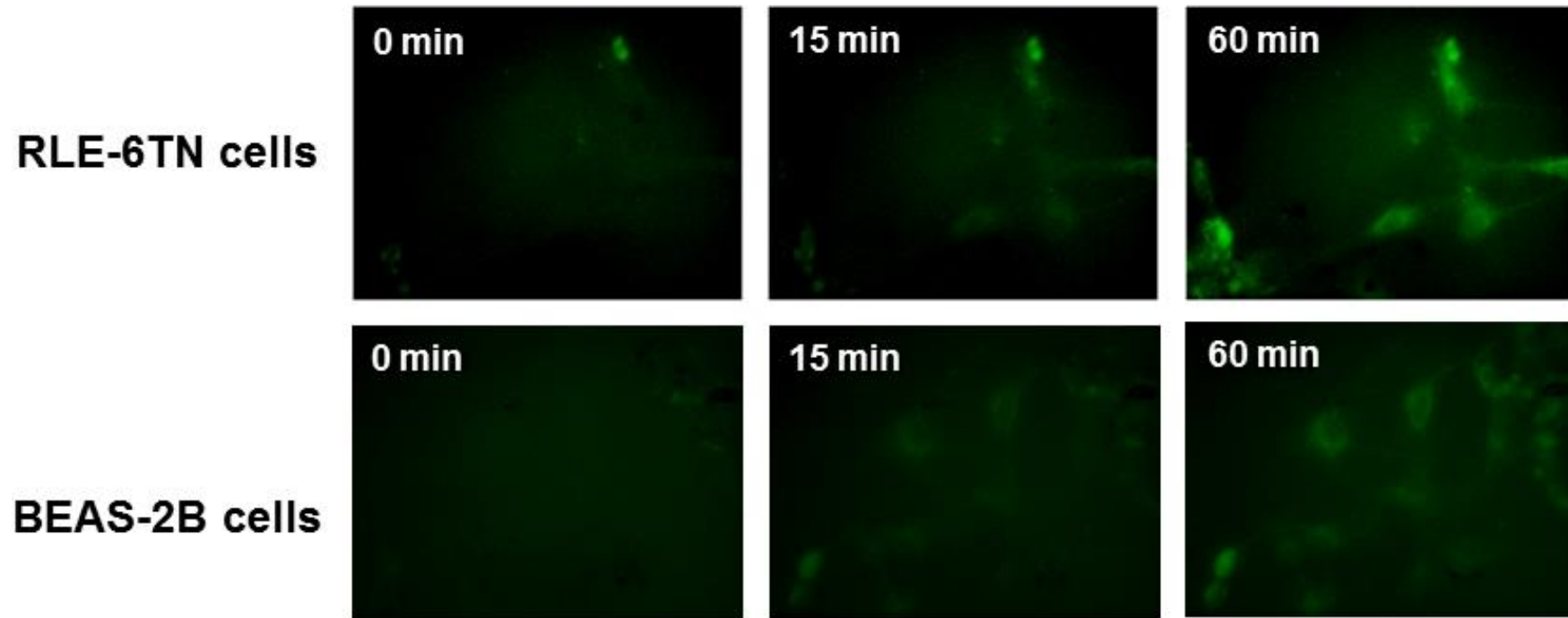


Fig. S6. Time-dependent accumulation of exogenous irisin in RLE-6TN and BEAS-2B cells. Cells were subjected to 2 hours of anoxia, and exogenous irisin (0.1 $\mu\text{g/ml}$) was added at time 0 min during the period of reoxygenation. The dynamic accumulation of irisin was observed by a time-lapse live cell system. See also **movies S1 to S3**.

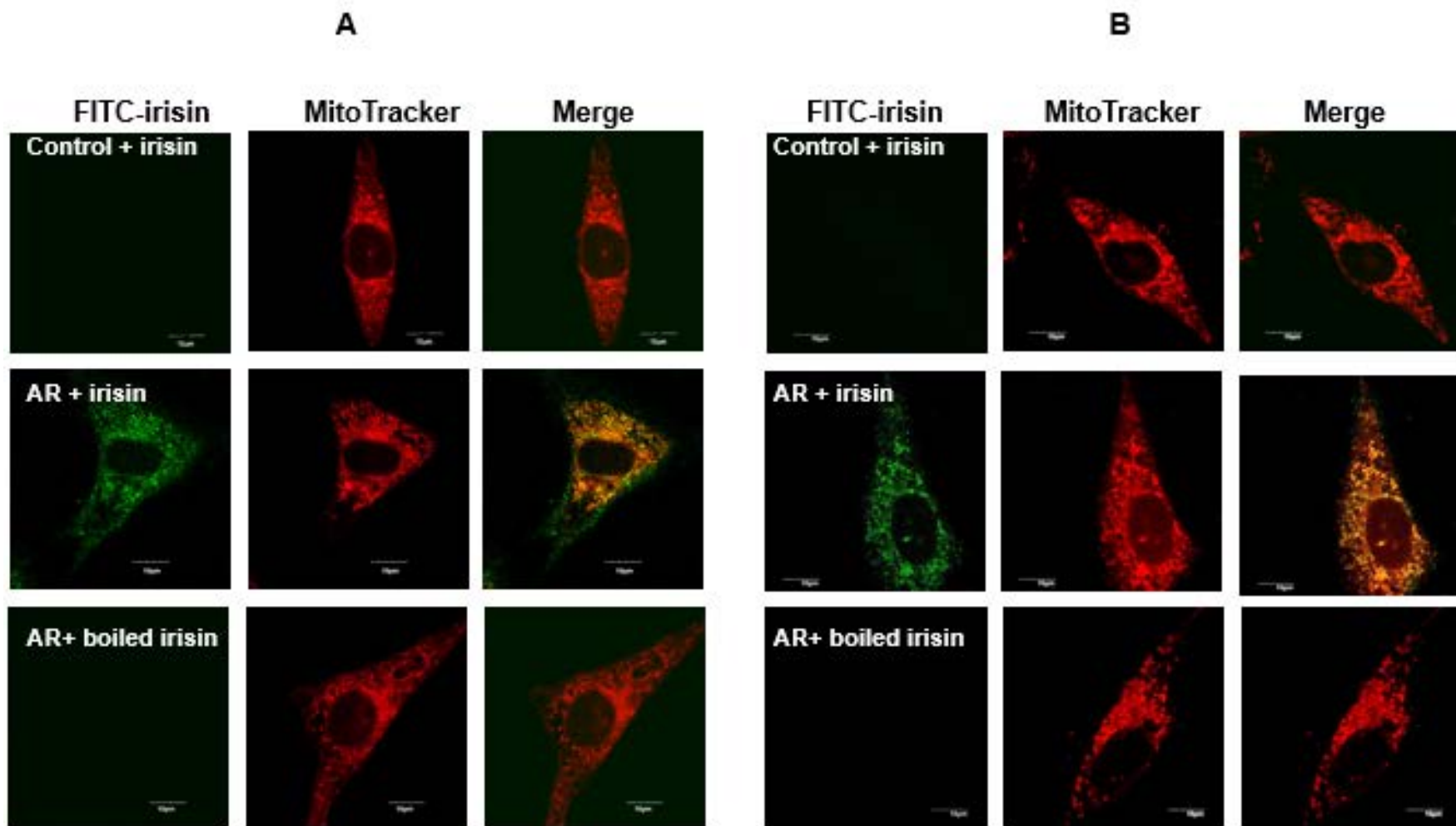


Fig. S7. Localization of irisin in mitochondria of cultured lung epithelial cells. Colocalization of irisin and MitoTracker Red was observed after AR injury in RLE-6TN cells (A) and BEAS-2B cells (B). Scale bar = 10 μ m. Boiled irisin was used as a negative control.

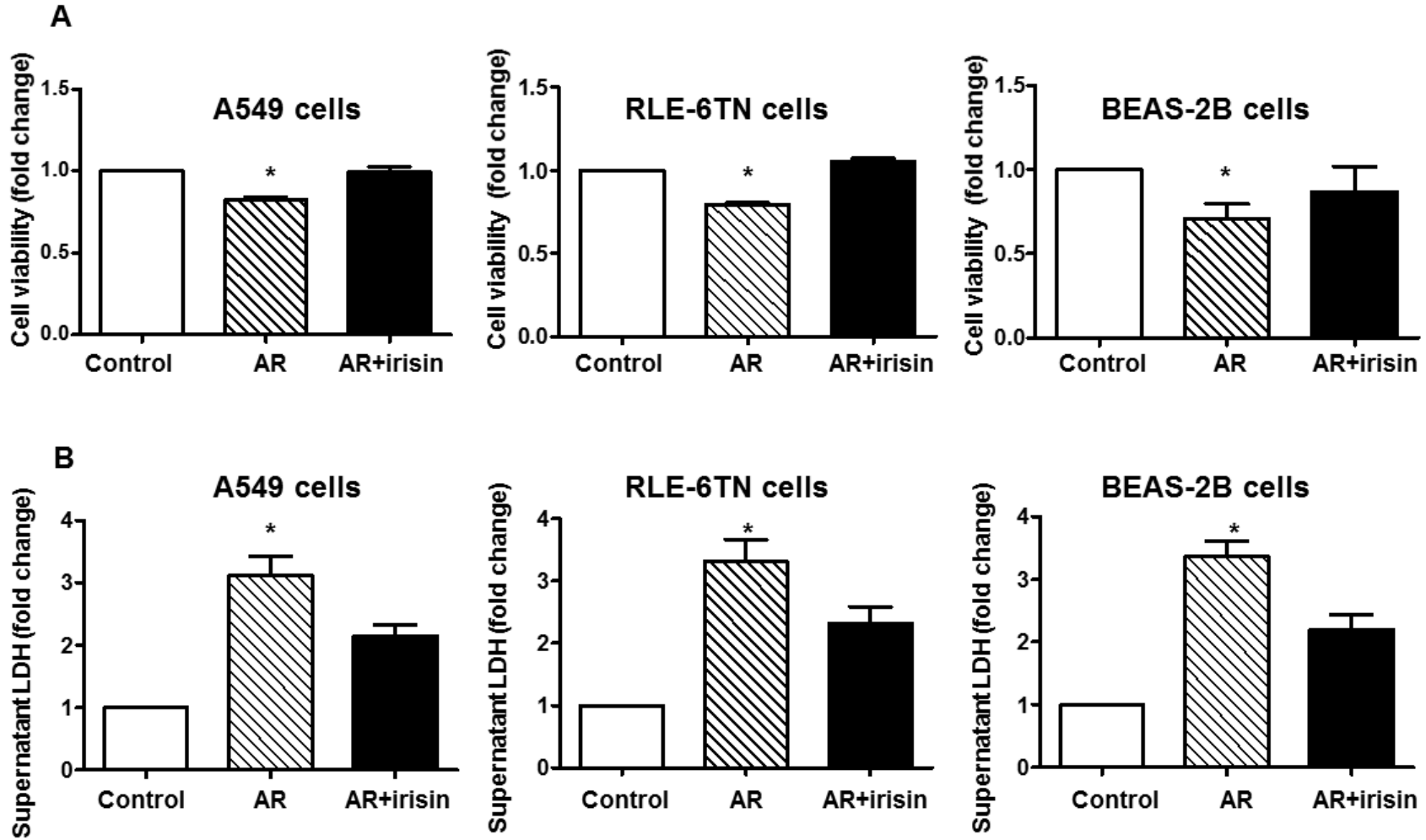


Fig. S8. Measurement of cell viability and LDH concentration in culture medium derived from lung epithelial cells after AR. Cell viability (A) was measured by cck-8 assay (* $P < 0.05$ vs. others, $n = 10$). LDH concentrations in cell supernatant (B) were measured by ELISA (* $P < 0.05$ vs. others, $n = 8$).

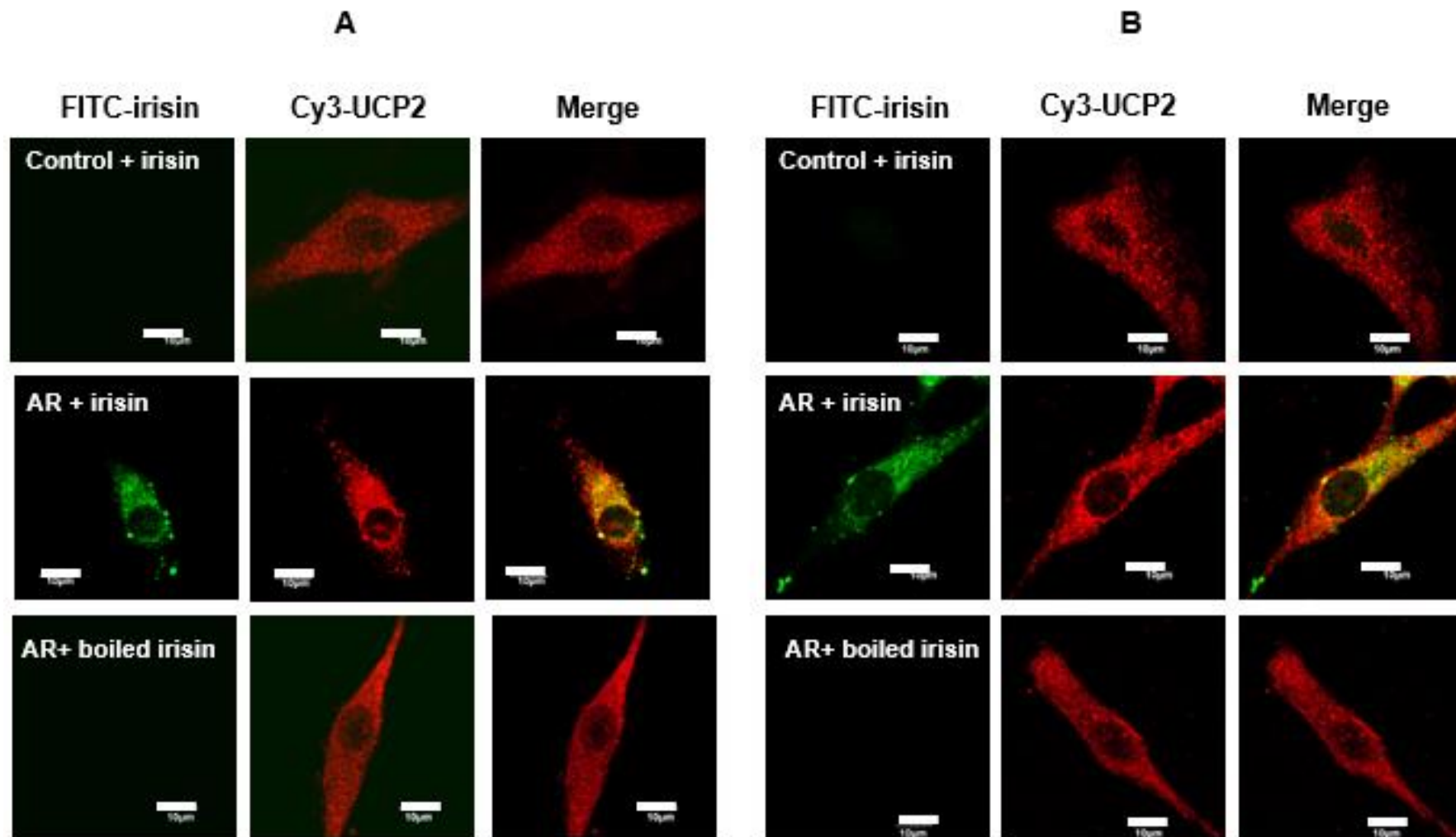


Fig. S9. Colocalization of irisin and UCP2 in lung epithelial cells. RLE-6TN cells (A) or BEAS-2B cells (B) were first treated with FITC-irisin (0.1 µg/ml) or FITC-boiled irisin and then immunostained with anti-UCP2 antibody. Co-localization of irisin and UCP2 was observed after AR injury (scale bar=10 µm).

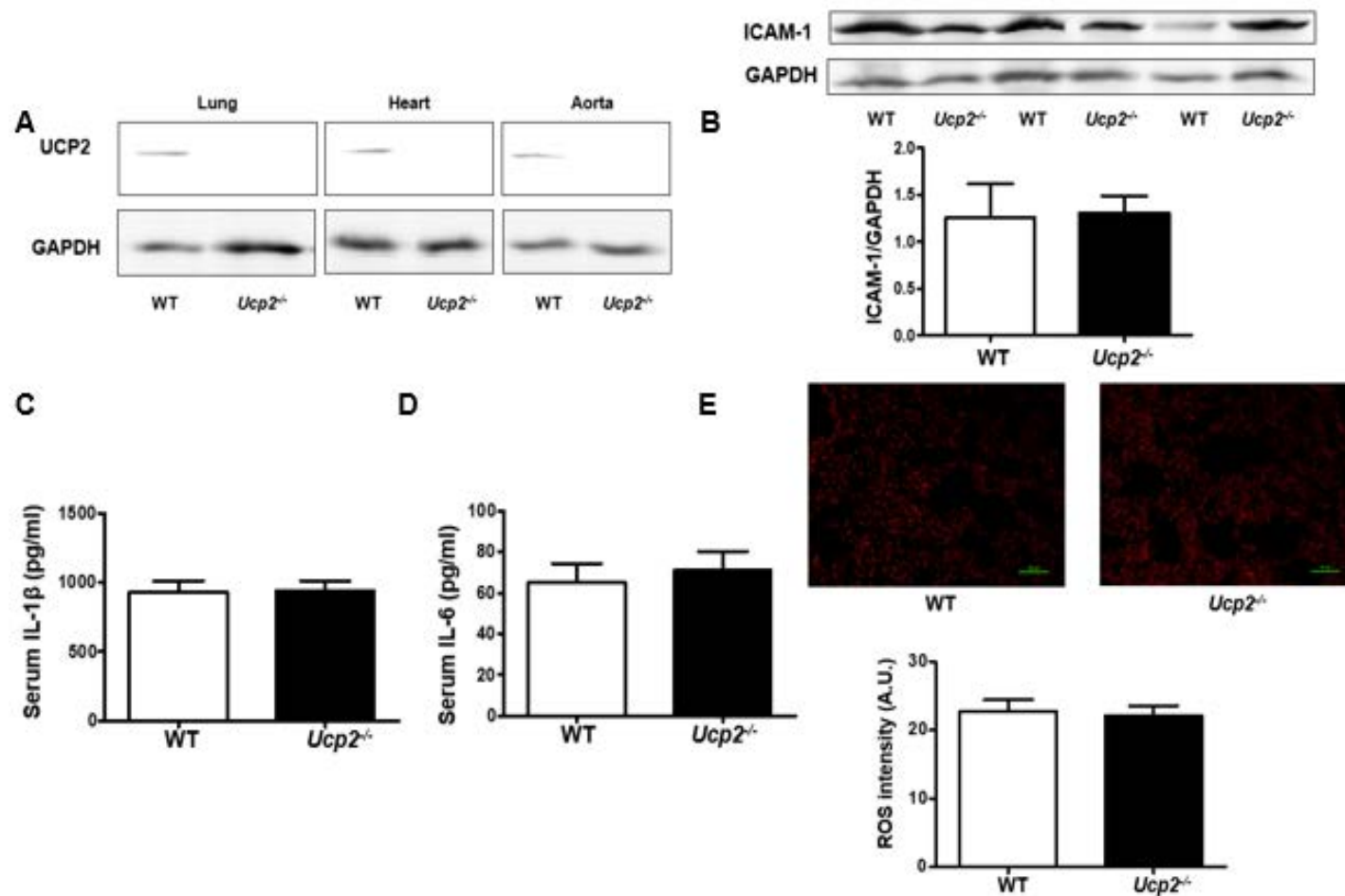


Fig. S10. Basal UCP2 expression, inflammation markers, and amount of ROS in WT and *Ucp2*^{-/-} mice. (A) UCP2 expression in lung, heart, and aorta tissues from WT and *Ucp2*^{-/-} mice. The 33 kDa UCP2 band was absent in samples from *Ucp2*^{-/-} mice. (B) The expression of intercellular cell adhesion molecule-1 (ICAM-1) was analyzed by immunoblotting (n=3, no significant difference). (C and D) Serum concentrations of IL-1 β (C) and IL-6 (D) were analyzed by ELISA (n=5, no significant difference). (E) ROS in lung section was measured by DHE staining. (n=4, no significant difference, scale bar= 50 μ m).

Table S1. The characteristics of control and NRDS newborn patients in Fig. 2B.

Control							NRDS						
No	ID	Gender	Gestational age (weeks)	Birth weight (kg)	5 min Apgar score	SpO ₂	ID	Gender	Gestational age (weeks)	Birth weight (kg)	5 min Apgar score	SpO ₂	
												Acute illness	Recovery
1	204970765	M	36	3.22	9	99	203477281	M	31	2.68	6	87	94
2	203478538	M	35	3.73	10	93	204267990	F	40	2.53	7	76	91
3	20498463	F	40	3.74	10	96	204941319	F	31	3.25	7	82	96
4	202414406	F	31	2.28	10	95	202422049	M	28	1.05	8	82	93
5	204940206	F	37	3.06	9	96	204944863	F	27	3.1	7	77	89
6	203457888	F	30	3.47	8	97	204940384	M	28	3.32	7	85	91
7	204944774	F	31	2.72	9	94	202422144	F	36	2.65	6	90	96
8	204946287	M	33	3.12	10	98							
9	204946331	F	32	2.86	10	96							
10	204944827	M	29	3.4	9	98							
11	204941002	M	36	3.43	8	96							
12	202414644	F	29	3.46	9	96							
13	204940991	M	37	3.6	10	93							
14	204945174	M	33	3.65	9	97							
15	202486346	F	34	2.56	9	98							

The characteristics of 15 control infants and 7 NRDS patients were collected during acute illness and after recovery. The serum or BALF samples were used for the protein chip study shown in **Fig. 2B**.

Table S2. The characteristics of control and NRDS newborn patients in Fig. 2C.

Control							NRDS						
No	ID	Gender	Gestational age (weeks)	Birth weight (kg)	5 min Apgar score	SpO ₂	ID	Gender	Gestational age (weeks)	Birth weight (kg)	5 min Apgar score	SpO ₂	
												Acute illness	Recovery
1	204970765	M	36	3.22	9	99	203477281	M	31	2.68	6	87	87
2	202414406	F	31	2.28	10	95	204267990	F	40	2.53	7	76	76
3	204946331	F	32	2.86	10	96	204941319	F	31	3.25	7	82	82
4	204941002	M	36	3.43	8	96	202422049	M	28	1.05	8	82	82
5	202414644	F	29	3.46	9	96	204940384	M	28	3.32	7	85	85
6	204945174	M	33	3.65	9	97	202422144	F	36	2.65	6	90	90

6 of the 15 control infants and 6 of the 7 NRDS patients were included in the LC-MS study (**Fig. 2C**). Characteristics of the 6 control infants and 6 NRDS patients during acute illness and after recovery are shown here.

Legends for Supplemental Movies

Movie S1. Uptake of exogenous irisin into BEAS-2B cells. FITC-irisin (0.1 $\mu\text{g/ml}$) in cell culture medium can translocate into the cytoplasm of BEAS-2B cell after 2-hour anoxia during the period of reoxygenation. Images were acquired at a rate of 2 min/frame.

Movie S2. Uptake of exogenous irisin into RLE-6NT cells. FITC-irisin (0.1 $\mu\text{g/ml}$) in cell culture medium can translocate into the cytoplasm of RLE-6NT cell after 2-hour anoxia during the period of reoxygenation. Images were acquired at a rate of 2 min/frame.

Movie S3. Uptake of exogenous irisin into A549 cells. FITC-irisin (0.1 $\mu\text{g/ml}$) in cell culture medium can translocate into the cytoplasm of A549 cell after 2-hour anoxia during the period of reoxygenation. Images were acquired at a rate of 2 min/frame.